2002

Insights into the Mechanism for Orogen-Related Carbonate Remagnetization from Growth of Authigenic Fe-Oxide: A Scanning Electron Microscopy and Rock Magnetic Study of Devonian Carbonates from Northern Spain

Arlo Brandon Weil
Bryn Mawr College, aweil@brynmawr.edu

Rob Van der Woo

Custom Citation

Weil, A. B., and R. Van der Voo (2002) Insights into the mechanism for orogen-related carbonate remagnetization from growth of authigenic Fe-oxide: A scanning electron microscopy and rock magnetic study of Devonian carbonates from northern Spain, *J. Geophys. Res.* 107, 2063.

JOURNAL OF GEOPHYSICAL RESEARCH, VOL. 107, NO. B4, 2063, 10.1029/2001JB000200, 2002

Insights into the mechanism for orogen-related carbonate remagnetization from growth of authigenic Fe-oxide: A scanning electron microscopy and rock magnetic study of Devonian carbonates from northern Spain

Arlo B. Weil[1] and Rob Van der Voo

Department of Geological Sciences, University of Michigan, Ann Arbor, Michigan, USA

Received 20 September 2000; revised 13 September 2001; accepted 1 October 2001; published 12 April 2002.

[1] A rock magnetic and SEM study of Devonian carbonates from the Cantabria-Asturias Region, northern Spain, was undertaken to further our understanding of the pervasive remagnetization of carbonate rocks during the Late Paleozoic, and the mechanism by which these remagnetizations occur. These rocks contain three ancient Late Paleozoic magnetizations. The rock magnetic properties of mineral extracts were compared with those of whole rock chips and "nonmagnetic" residue to deduce magnetic carrier(s) and grain sizes. Hysteresis measurements for rock chips show "typical" wasp-waisted loops, whereas extract shows typical pseudosingle-domain-like (PSD) unrestricted loops. Within all sites, there is a noticeable contribution of superparamagnetic (SP) grains seen in hysteresis properties and low-temperature magnetization measurements of whole rock chips, whereas a trend away from a strong SP contribution is seen when hysteresis properties of whole rock are compared with those of residue and extract. Consequently, our extraction process (predictably) removes SP grains, while preserving the characteristic fraction of remanence-carrying material, which behaves like a typical mixture of single-domain (SD) and PSD magnetite. Paradoxically, the typical "fingerprint" of remagnetized carbonates, as seen in the whole rock data, seems to be a response to abundant SP grains associated with the acquisition of chemical remanent magnetizations (CRM), and not the actual remanence carrying population itself. Scanning electron microscopy (SEM) observations of magnetic extract reveal abundant authigenic Fe-oxides, characterized as either 10–100 μm Ni-free spherules or individual 0.1–10 μm euhedral grains. SEM observations of thin sections reveal abundant evidence of fluid flow driven chemical reactions that resulted in formation of new Fe oxide. Such reactions occurred along cracks and grain boundaries and within void space, and are associated with Fe-rich clay and calcite-dolomite reactions or as oxidation of Fe-sulfide framboids. Together, the SEM observations and rock magnetic experiments reveal that the three Late Paleozoic remagnetizations experienced by Cantabria-Asturias Paleozoic carbonates are CRMs facilitated by the presence of fluids activated during Late Paleozoic Variscan deformation. *INDEX TERMS:* 1533 Geomagnetism and Paleomagnetism: Remagnetization; 1540 Geomagnetism and Paleomagnetism: Rock and mineral magnetism; 1527 Geomagnetism and Paleomagnetism: Paleomagnetism applied to geologic processes; 1525 Geomagnetism and Paleomagnetism: Paleomagnetism applied to tectonics (regional, global); *KEYWORDS:* Remagnetizations, carbonates, Variscan, Cantabria-Asturias Arc, rock magnetism, magnetic extraction

1. Introduction

[2] The final amalgamation of Pangea during the Late Paleozoic Variscan-Alleghanian orogeny is widely recognized as having caused global-scale remagnetizations. Although mostly reported in limestones, this event affected many types of sedimentary rocks in all of Pangea's major blocks (Figure 1), including, but not limited to, North America, Europe, Asia, Africa, and Australia. The ubiquity of these remagnetizations has led to considerable rock magnetic research focused on the possible cause(s) and carrier(s) of this pervasive event. Two main mechanisms have been proposed for the remagnetization of Paleozoic limestones: (1) the acquisition of a thermoviscous remanent magnetization (TVRM) caused by burial and prolonged exposure to elevated temperatures [*Kent*, 1985] and (2) the acquisition of a secondary chemical remanent magnetization (CRM) through magnetic mineral growth activated by basinal brines and other orogenic fluids [e.g., *McCabe et al.*, 1983; *Bachtadse et al.*, 1987; *Jackson*, 1990; *Suk et al.*, 1990a; *Thominski et al.*, 1993; *Molina-Garza and Zijderveld*, 1996]. It is now widely believed that secondary CRMs are the cause of most Paleozoic carbonate remagnetizations and that TVRMs are unlikely given the relatively low burial temperatures determined for carbonates studied (<250°C). Although the ubiquity of this process is widely accepted, the mechanism for the remagnetizations, and its relationship with orogeny, is still not fully understood. To further our understanding, details of mineralogy and genesis of CRM carriers must be determined. Ultimately, a better understanding of the origin and distribution of natural remanent magnetization (NRM) carriers will allow comparison between affected Paleozoic carbonates

[1]Now at Department of Geology, Bryn Mawr College, Bryn Mawr, Pennsylvania, USA.

0148-0227/02/2001JB000200$09.00

Figure 1. Map of Pangea showing extent of Late Paleozoic carbonate remagnetization. Dots represent published Paleozoic carbonate formations remagnetized during the Late Carboniferous–Early Permian Variscan–Alleghanian coeval orogenies.

from varying localities to determine whether they have acquired similar CRMs in response to the Late Paleozoic Variscan-Alleghanian orogeny and, as a result, whether remagnetized carbonates share a common rock magnetic signature and remagnetization history.

[3] Previous studies of remagnetized North American platform carbonates suggest that they hold a magnetic "fingerprint" that distinguishes them from unremagnetized carbonates and synthetic samples of mixed magnetite grain sizes [*Jackson*, 1990; *McCabe and Channell*, 1994; *Channell and McCabe*, 1994]. Of these signatures, hysteresis properties have been the most universal, with typical remagnetized limestones having anomalously high Hcr/Hc ratios with respect to given Mrs/Ms ratios. Such high Hcr/Hc ratios are typically associated with bimodal distributions of vastly different magnetic coercivity phases caused by mixtures of either grain size (i.e., a combination of superparamagnetic (SP) and single-domain (SD) grains) [*Pick and Tauxe*, 1993; *Tauxe et al.*, 1996], magnetic mineralogy (i.e., magnetite and hematite) [*Roberts et al.*, 1995; *Muttoni*, 1995], or particle anisotropy (both shape and magnetocrystalline) [*Jackson*, 1990]. These contrasting coercivity distributions commonly result in wasp-waisted hysteresis loops [*Wasilewski*, 1973], which have been proposed as one of the more recognizable signatures of remagnetized carbonates [*Jackson*, 1990; *McCabe and Channell*, 1994; *Channell and McCabe*, 1994]. Unfortunately, it is very difficult and often impossible to use wasp-waisted hysteresis loops for direct interpretation of magnetic grain size and mineralogy [*Tauxe et al.*, 1996]. Consequently, because of the inherent nonuniqueness in hysteresis parameter interpretation [*Parry*, 1982] a definitive explanation for the pervasiveness of wasp-waisted hysteresis loops in remagnetized carbonates, and subsequently the existence of a magnetic fingerprint, has been elusive.

[4] To better understand the origin and global predominance of the Late Paleozoic remagnetization event and its proposed fingerprint on carbonates, we undertook a study of remagnetized Devonian carbonates from the Cantabria-Asturias Arc (CAA), northern Spain (Figure 2). This area is paleomagnetically unique in that the Paleozoic rocks have experienced several sequential remagnetizations during the Variscan-Alleghanian orogeny. To characterize the distribution of crystal morphology and granulometry and to determine in which minerals the magnetic remanence resides, rock magnetic properties of whole rock chips are compared with those of magnetic extracts and "nonmagnetic" residue. These rock magnetic properties include hysteresis parameters, demagnetization of three-dimensional (3-D) isothermal remanent magnetization (IRM), acquisition of IRM, saturation IRM (SIRM), and anhysteretic remanent magnetization (ARM), and low-temperature demagnetization. To describe the morphology and chemical composition of the magnetic grains present, scanning electron microscopy (SEM) was used on magnetic extract and thin sections.

[5] Collectively, the rock magnetic and SEM results provide identification of the mineralogy and grain size of remanence carriers in CAA carbonates, and determination of the source for the rock magnetic fingerprint found in remagnetized carbonates. Furthermore, by comparing the rock magnetic behavior of suites of rocks that carry different remagnetization components, we are able to determine whether different remagnetization components found in the same formation have distinguishing rock magnetic characteristics and therefore experienced distinctive remagnetization histories. Last, we are able to use these results to elaborate on the mechanism of attaining several remagnetizations so close in time and space and on the relationship between remagnetization events, regional deformation, and global tectonic events.

2. Geologic and Paleomagnetic Background

[6] The CAA of northern Spain is a unique orogenic belt in that it displays 180° of arc curvature that is concave toward the orogenic foreland; that is, fold-thrust vergence is toward the core of the arc (Figure 2). Recently, *Weil et al.* [2000] undertook a detailed paleomagnetic study of two Devonian limestone formations (the Santa Lucia and Portilla formations) within individual structural domains of the CAA hinge zone to determine the geometry and timing of Variscan deformation and elucidate regional structural characteristics. Results of that study suggest

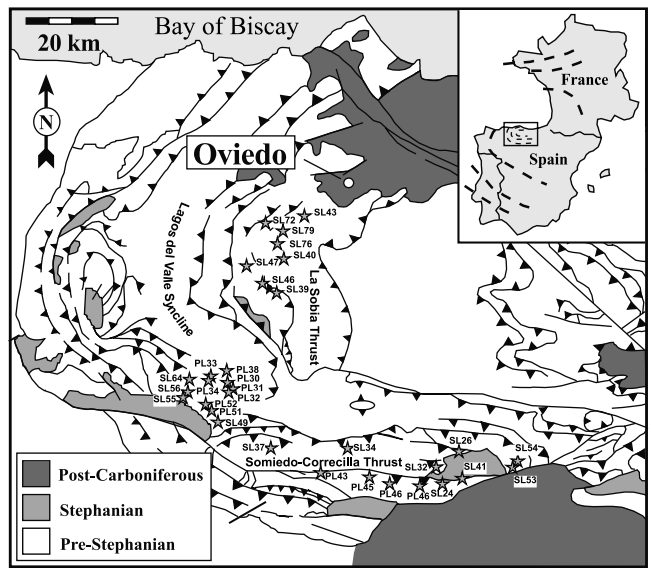

Figure 2. Schematic structural map of the Cantabria-Asturias Arc, northern Spain, with insert showing its position in the larger Ibero-Armorican Arc. Stars represent site locations for the samples used in this study.

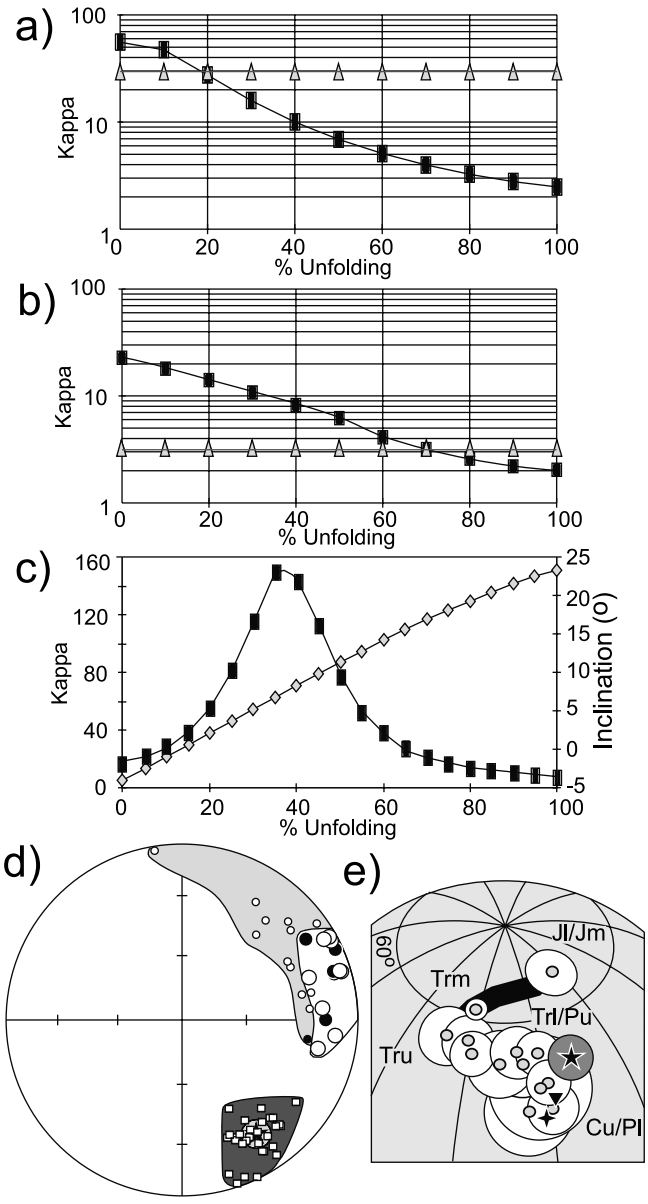

Figure 3. (a) Regional incremental fold test of the PT remanence carrying sites plotting kappa (squares) and critical ratio (CR) (triangles) versus percent unfolding. (b) An example of a B component regional incremental fold test from the southern limb of the CAA indicating a posttilting magnetization acquisition. The CR parameter is the critical ratio above which kappa becomes significant at the 95% confidence level. (c) An example of a C component inclination-only fold test from the hinge zone of the CAA, indicating a synfolding magnetization acquisition. Percent unfolding is plotted against kappa (squares) and inclination (diamonds). (d) Stereonet of in situ PT (squares within dark shaded envelope), B (large circles within open envelope), and C (small circles within shaded envelope) component site means from the southern limb of the CAA. Open symbols represent upper hemisphere projections. Star and shaded circle represent mean direction and its associated alpha 95, respectively. (e) A portion of Iberia's APWP for the Late Paleozoic and early Mesozoic showing the position of the in situ PT (five-sided star), and structurally corrected B (inverted triangle) and C (four-sided star) remagnetization poles.

that the CAA curvature is related to a change in the regional stress field, from earlier dominantly east-west compression to later north-south compression, caused by the lock-up of Iberia between Laurussia and Gondwana during the final amalgamation of Pangea.

[7] The samples used for this study were taken from the collection of Devonian carbonates used by *Weil et al.* [2000] in the hinge zone as well as other samples collected in the southern limb of the CAA [*Weil et al.*, 2001]. The two formations sampled reveal three ancient remagnetizations, and individual samples may carry one or two of these. In all cases the magnetization components were distinguished by their relationship with deformation events, which was determined by local and regional fold tests (Figure 3) [see also *Weil et al.*, 2000, 2001]. These components and their relationship to deformation are a previously unrecognized postorogeny Late Permian-Early Triassic (PT) component with southeast declinations and intermediate up inclinations (Figure 3), a posttilting yet prerotation Early Permian (B) component with shallow inclinations, and a Late Carboniferous synfolding (C) component. A low unblocking temperature viscous present-day field overprint (component A) was found in all samples (northerly and down) and was removed by 250°C. The distinction of the PT component as postdeformational was determined by fold tests and comparing the in situ paleopole position calculated from 30 paleomagnetic sites located in the southern zone of the CAA with stable Iberia's Late Paleozoic and Mesozoic apparent pole wander path (APWP) (Figure 3) [*Parés et al.*, 1996]. The PT component was not found in the CAA hinge zone. Demagnetization plots for representative samples from the entire study area are shown in Figure 4.

[8] The geographical distribution of magnetization components within the CAA indicates a regional tectonic control on remagnetization, i.e., possible fluid migration along major structural detachments. The B magnetization is present throughout the hinge area of the arc, whereas the C magnetization is restricted to the outer thrust unit only, and the youngest PT component is restricted to the southern belt only. Paleotemperature maps, based on the conodont alteration index of the sample area [*Raven and Van der Pluijm*, 1986; *Bastida et al.*, 1999], also show a correlation with major structural features. This led *Raven and Van der Pluijm* [1986] to conclude that the structurally controlled temperature domain boundaries were caused by orogenic fluids associated with hinterland activity, which by inference is likely linked to the CAA remagnetization history. *Van der Voo et al.* [1997] suggested that a similar rock-fluid interaction could have been the remagnetizing mechanism in the CAA's Lagos del Valle Syncline. It should be noted that paleotemperature estimates for the studied area never exceeded ~250°C, which likely rules out TVRMs being responsible for the CAA multiple remagnetizations.

3. Sampling and Methods

3.1. Sampling

[9] Oriented cores were collected for paleomagnetic analysis with a portable gas-powered drill at over 200 sites in 1996, 1997, and 1999. Samples from a total of 37 sites were chosen from this collection based on their previously determined paleomagnetic behavior (i.e., how many and which magnetic components were observed) (Figure 2). Details of the samples' rock magnetic and paleomagnetic properties can be found in the data repository (see Table A1[1]).

3.2. Magnetic Extraction

[10] Given the low concentration of magnetic minerals in CAA limestones, magnetic extraction was completed to concentrate

[1]Supporting Table A1 is available via Web browser or via Anonymous FTP from ftp://agu.org, directory "apend" (Username = "anonymous", Password = "guest"); subdirectories in the ftp site are arranged by paper number. Information on searching and submitting electronic supplements is found at http://www.agu.org/pubs/esupp_about.html.

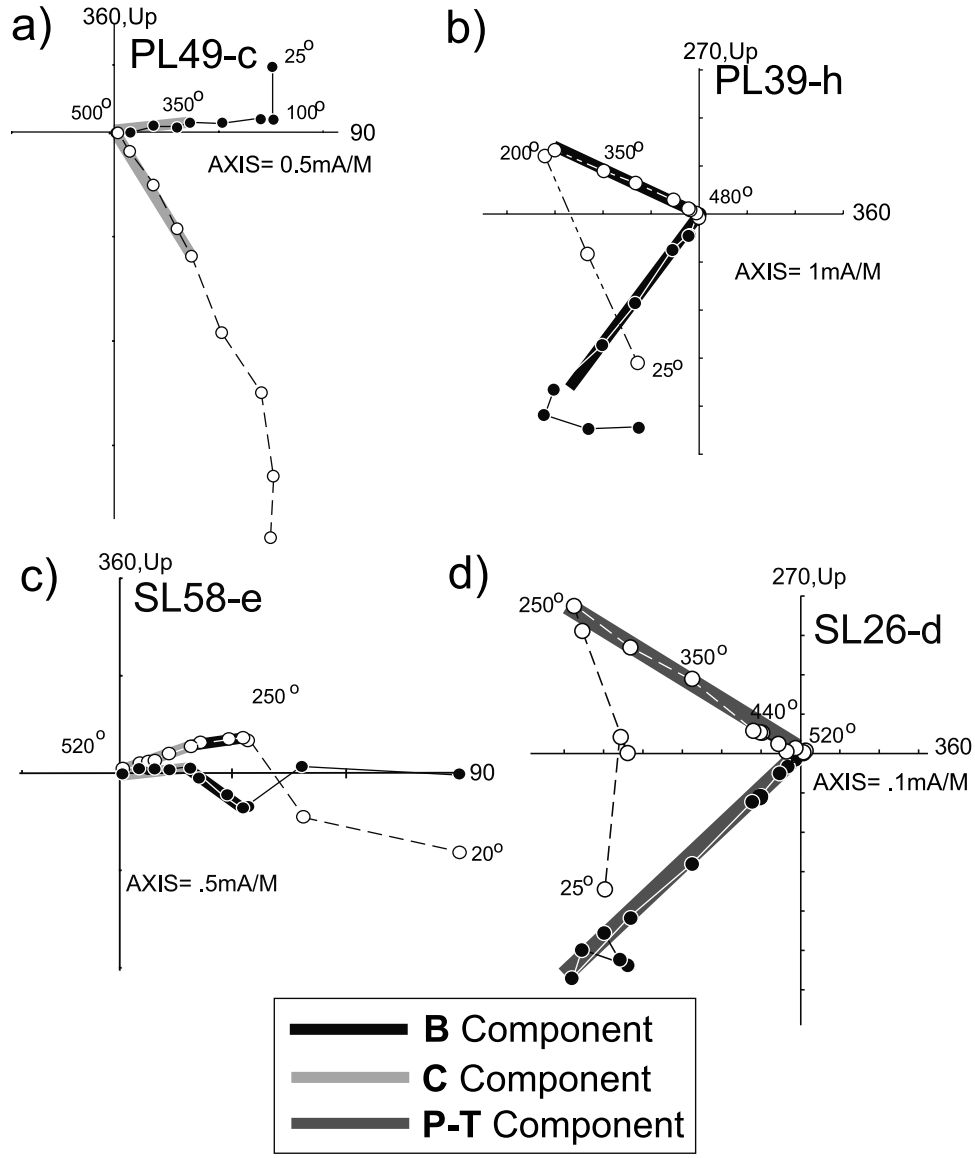

Figure 4. Typical examples of orthogonal projection plots in in situ coordinates showing the ancient remagnetization components held by CAA carbonates: (a) C component, (b) B component, (c) B and C components, and (d) PT component. Open circles represent projections onto the vertical plane; solid circles represent projections onto the horizontal plane. Thermal demagnetization temperatures are given in degrees Celsius.

magnetic material for both rock magnetic measurements and SEM analysis. For each site a core was also set aside for bulk rock measurements and thin section preparation. The remaining cores for each site were sliced into thin (<1 cm) disks using a non-magnetic rock saw and bathed for several minutes in a 10% HCl solution to remove any contamination from drilling, sawing, and handling. After thorough rinsing of the disks with deionized water, each was placed in an ultrasound bath for several minutes and then dried. When cleaning was complete, the disks were ground down in a slam-jaw rock crusher until all fragments were <1 mm and then transferred to a wolfram-carbide shatter box and further crushed until the powder had particle sizes <100 μm. During the crushing process, "dummy" samples (CAA carbonate rock chips not used in this study) were crushed and tested for metal and steel fragment contamination using a magnet placed under the crushed rock. No visible contamination from the crushers was found. Both rock-crushing devices were cleaned with ethyl alcohol between sample processing.

[11] The crushed samples, which averaged 250 mg, were subsequently placed in cleaned 600-mL glass beakers under a fume hood and slowly mixed with a solution of 1 N acetic acid buffered with sodium acetate to a pH of 4.0. It has been shown [*McCabe et al.*, 1983; *Freeman*, 1986] that this solution is properly buffered to minimize the effects of magnetic mineral alteration and optimize carbonate dissolution efficiency. The rock powder-acid mixture was stirred several times a day to stimulate carbonate dissolution and then left to settle overnight. The remaining acid was decanted every morning with a cleaned syringe and replaced with a new buffered acetic acid solution. This process was repeated daily for up to 10 weeks, until all carbonate was dissolved. The remaining slurry was then cleaned several times with deionized water until all remains of the acid solution were removed. Thereafter, samples were dehydrated in a freeze-drier and mixed with an anticoagulant (e.g., calgon) to disperse the fine-grained particles, in particular, the large amount of clay particles present. The final step before magnetic mineral

extraction was to place the samples into an ultrasonic bath for several minutes to further decoagulate the slurry.

[12] As described by *Freeman* [1986], a Franz electromagnet was configured so that the pole faces were positioned vertically to allow passage of the sediment-rich slurry for magnetic mineral extraction. A Tygon™ tube was attached to a stopgap below a slurry reservoir placed above the electromagnet. The tube was then run through a peristaltic pump and back into the slurry reservoir to form a closed circuit. The peristaltic pump was set at a flow rate between 1 and 3 cm^3/min to allow fine magnetic mineral migration to the sides of the magnetic poles during pumping. The current to produce the electromagnetic field was set at 0.20 A, yielding approximately a 0.10 T field. After a 24-hour cycle the stopgap was closed, and deionized water was flushed through the tube to clean out any extra residue buildup. Care was taken to prevent air bubbles from entering the tube with the deionized water, as surface tension gradients would cause extract to be stripped from the tube walls. After sufficient cleaning, the section of tube between pole faces was removed, and the magnetic extract was flushed into 50-mL beakers until the tube walls were cleaned. The beakers were then placed in a drying oven until all water was evaporated, and the magnetic extract had settled to the bottom of the beakers. The samples were doused with a small amount of deionized water, placed in an ultrasonic bath and transferred to cleaned 10-mL plastic sample holders to dry. This procedure produced a highly concentrated magnetic extract, which could be used for both rock magnetic and SEM study. Finally, the nonmagnetic residue for each site was cleaned, dried, and weighed for rock magnetic experiments run in parallel with whole rock chips and extract.

3.3. Rock Magnetism

[13] Hysteresis properties of magnetic extract, nonmagnetic residue and bulk rock were measured with a Princeton Vibrating Sample Magnetometer (Micro-VSM) at the Institute for Rock Magnetism at the University of Minnesota. Low-temperature magnetic behavior of bulk rock and nonmagnetic residue was measured using a Quantum Design MPMS2 cryogenic magnetometer, also at the Institute of Rock Magnetism. Acquisition and demagnetization of saturation isothermal remanent magnetization (SIRM) and anhysteretic remanent magnetization (ARM) were measured in the University of Michigan's paleomagnetic laboratory. IRMs were imparted with an electric magnet in fields up to 1.2 T. ARMs were imparted in AC fields up to 200 mT, with a DC bias field of 0.5 mT. Finally, thermal demagnetization of three-axis IRM [*Lowrie*, 1990] was performed on representative samples based on their IRM acquisition curves and low-temperature behavior. For the three-axis measurements an IRM was first imparted down the long axis of the cores (z axis) with the maximum available field of 1.2 T. Subsequently, 0.4-T and 0.12-T fields were applied along the x and y axis, respectively.

3.4. SEM

[14] After all rock magnetic experiments were complete, magnetic extract and cores of representative samples were prepared for analysis with the scanning electron microscope (SEM). Magnetic extract was dusted onto carbon tape and carbon coated. Paleomagnetic cores were mounted for thin section preparation and carbon coated. Energy-dispersive spectral analysis (EDS) and photographs were taken with a Hitachi S-570 SEM fitted with a backscattered electron (BSE) detector and a Kevex Quantum detector.

4. Results

4.1. IRM Acquisition and Three-Axis IRM Demagnetization

[15] IRM measurements were made on core specimens from 34 of the 37 sites studied (Figure 5). In 23 of the 34 samples

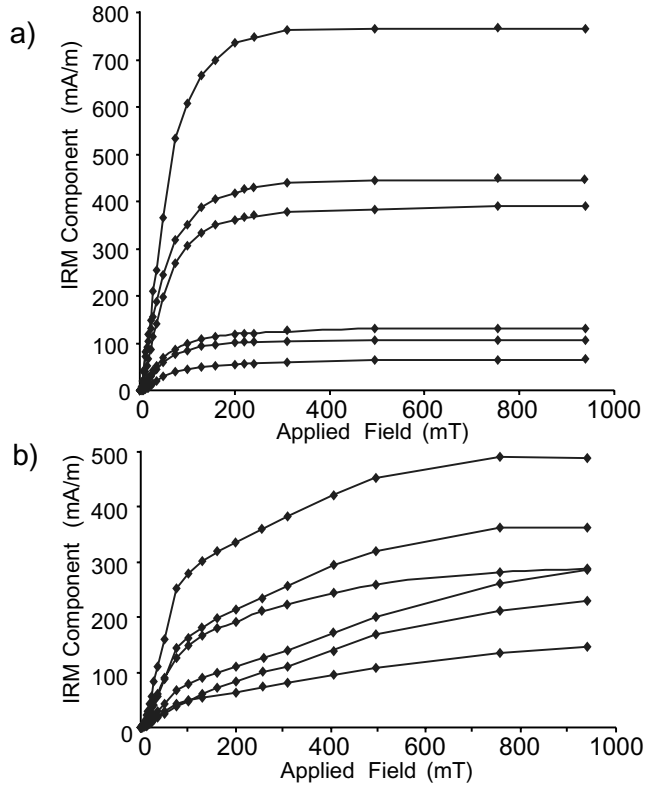

Figure 5. Typical IRM acquisition curves for samples containing (a) only low-coercivity mineral phases and (b) low- and high-coercivity mineral phases.

measured, IRM was acquired rapidly in low fields (<0.2 T), becoming completely saturated by 0.3 T, indicating a dominance of low- to medium-coercivity mineral phases. In the remaining 11 samples, IRM was again acquired rapidly in low fields (<0.2 T); however, a higher-coercivity mineral phase was present that could not be saturated with the available fields. Hematite and/or goethite are likely candidates for these higher-coercivity phases.

[16] To test this hypothesis, thermal demagnetization of three-axis IRM was performed according to the method of *Lowrie* [1990] (Figure 6). With this technique, magnetic minerals with contrasting coercivities can be identified according to their respective unblocking temperatures. Twelve representative samples were chosen based on IRM acquisition curve behavior: six samples that were completely saturated by 0.3 T and six samples that carried a higher-coercivity phase. The dominant magnetic mineral present is a low- to medium-coercivity phase, likely magnetite, which confirms the results obtained from IRM acquisition (Figure 6a). In all cases, ~85% of the total IRM was removed by 550°C, and in all but one of the samples (Figure 6b), 95% of the soft coercivity component was removed by 500°C. The unblocking temperature of the soft component was very similar to the average unblocking temperature observed during NRM demagnetization. Of the six samples that carried the higher-coercivity phase, four had their medium and hard component unblock at 680°C, typical of hematite (Figure 6b), and two unblocked by 120°C, typical of goethite (Figure 6c). However, of the ~1700 carbonate cores thermally demagnetized for paleomagnetic purposes, less than one tenth of 1% had unblocking temperatures above 580°C. This suggests that although present as a magnetic phase, hematite is not a significant remanence carrier in CAA limestones. Typical goethite demagnetization behavior was never clearly observed. Together, unblocking temperatures of

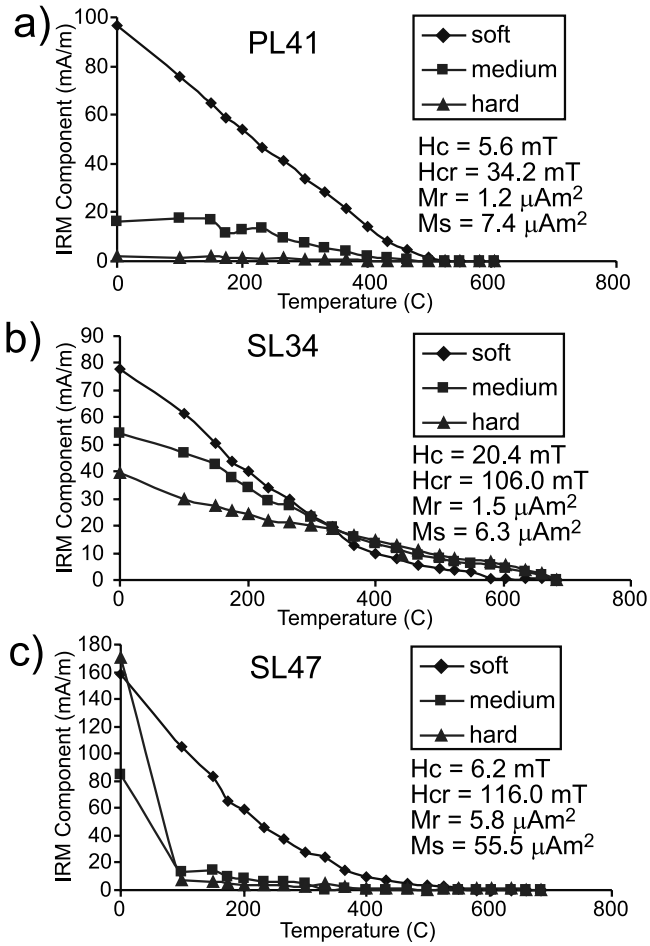

Figure 6. Typical measurements of thermal demagnetization of three-axis IRM for samples containing (a) magnetite only, (b) magnetite and hematite, and (c) magnetite and goethite. Thermal demagnetization of three-axis IRM produced by magnetizing the samples in a 1.2-T field along the *z* axis, followed by a 0.4-T field along the *y* axis, and finally a 0.12-T field along the *x* axis [*Lowrie*, 1990].

NRM, three-axis IRM, and IRM acquisition curves, all suggest that magnetite is the dominant carrier of CAA's ancient remagnetizations.

4.2. Hysteresis Measurements

[17] Hysteresis measurements were made on extract, nonmagnetic residue, and whole rock chips from each of the 37 sample sites, for a total of 111 measurements. Typical examples of all three sample sets are shown in Figure 7. Whole rock and several residue hysteresis loops indicated both diamagnetic and paramagnetic influences at high field strengths. Consequently, measurements were slope-corrected to remove effects of any nonferromagnetic and/or ferrimagnetic mineral phase. Several samples could not be saturated during hysteresis measurement, indicating the presence of a high-coercivity mineral phase. These samples were removed from analysis of hysteresis ratios.

[18] Measured Mr/Ms ratios from the saturated samples ranged between 0.03 and 0.24 for whole rock chips, 0.10 and 0.29 for residue, and 0.14 and 0.35 for extract (Figure 7). Measured Hcr/Hc ratios ranged between 3.4 and 18.9 for whole rock chips, 1.7 and 7.1 for residue, and 1.5 and 3.4 for extract (Figure 7). When ratios are plotted on Day diagrams [*Day et al.*, 1977], extract and residue values for Mr/Ms and Hcr/Hc lie mainly in the pseudosingle-domain (PSD) field and in the PSD and multidomain (MD) fields for whole rock chips. As has been found in almost all other studies of remagnetized limestones [*Jackson*, 1990; *McCabe and Channell*, 1994; *Channell and McCabe*, 1994], whole rock hysteresis loops for CAA carbonates were strongly wasp-waisted (Figure 7c). None of the extract loops showed any evidence of constricted hysteresis loops (Figure 7a).

[19] When hysteresis measurements are examined according to the magnetic component(s) held by the samples (Figure 8), groupings are observed, indicating that the magnetic behaviors of the different remagnetizations carry distinct fingerprints of the carbonates' history. Whole rock hysteresis properties have the most distinctive clusters of the different magnetization components (Figure 8a). The older magnetization (C) has the lowest Hcr/Hc ratios, while one of the younger magnetizations (B) has the highest Hcr/Hc ratios. Samples that carry both B and C magnetizations have intermediate values. The youngest of the three remagnetizations (PT) has a similar distribution to those samples that carry both the B and the C components.

4.3. Low-Temperature Demagnetization

[20] To further test the magnetic mineralogy present in CAA limestones, as well as test for the relative contribution of SP grains, samples from each site were given an IRM at room temperature, allowed to cool in a zero field (ZF) to 20 K, given an SIRM, and then warmed to room temperature in a zero field (Figures 9a–9c). Several samples were also field cooled (FC) in a 2.5-T field, and a second warm-up was run to test for the presence of goethite (Figures 9d and 9e). Six samples showed a classic Verwey transition at ~120 K (Figure 9b), indicating that magnetite is an important contributor to total IRM.

[21] Four samples showed the Morin transition at ~225 K during cooldown [*Liebermann and Banerjee*, 1971] (Figure 9c), which represents the presence of >0.1 μm hematite [*Bando et al.*, 1965]. The lower than normal temperature of the Morin transition, usually occurring near 260 K, is likely due to impurities and vacancies in the hematite crystal lattice or the lack of crystalinity [*Morrish*, 1994]. However, as determined from NRM demagnetization, hematite has negligible influence on the natural remanence in CAA carbonates.

[22] *Özdemir and Dunlop* [2000] documented that samples containing goethite experience a larger drop in total moment during warm-up after being field cooled compared to warm-up after being ZF cooled. This behavior is due to the large coercivity at low temperatures of goethite, which makes low-temperature magnetization very inefficient after zero field cooling. Confirming three-axis IRM demagnetization, the same samples that had medium- and high-coercivity phases unblock by 120°C exhibited a much larger difference in magnetic moment drop during warm-up after being field cooled compared to the difference after being zero field cooled (Figure 9d). Those samples that showed no evidence of goethite displayed more comparable warm-up curves after FC and ZF cooled runs (Figure 9e).

[23] Similar to observations made on remagnetized Paleozoic carbonates from Missouri [*Sun and Jackson*, 1994], a majority of CAA carbonate samples show a rapid loss of IRM intensity below 50 K during warming. This behavior strongly suggests a large population of SP grains [*Xu et al.*, 1998; *Katz et al.*, 1998a].

4.4. Cisowski Tests

[24] To further test the domain state, interactive nature, and grain size of the magnetic minerals, crossover plots were created comparing IRM acquisition curves with AF decay curves of IRM [*Cisowski*, 1981]. Figure 10 shows that AF decay of IRM is almost a mirror image of IRM acquisition, with both curves intersecting at ~50% normalized moment. According to *Cisowski* [1981] this behavior represents a population of noninteracting SD and/or PSD particles. The low fields between 40 and 60 mT at which crossover

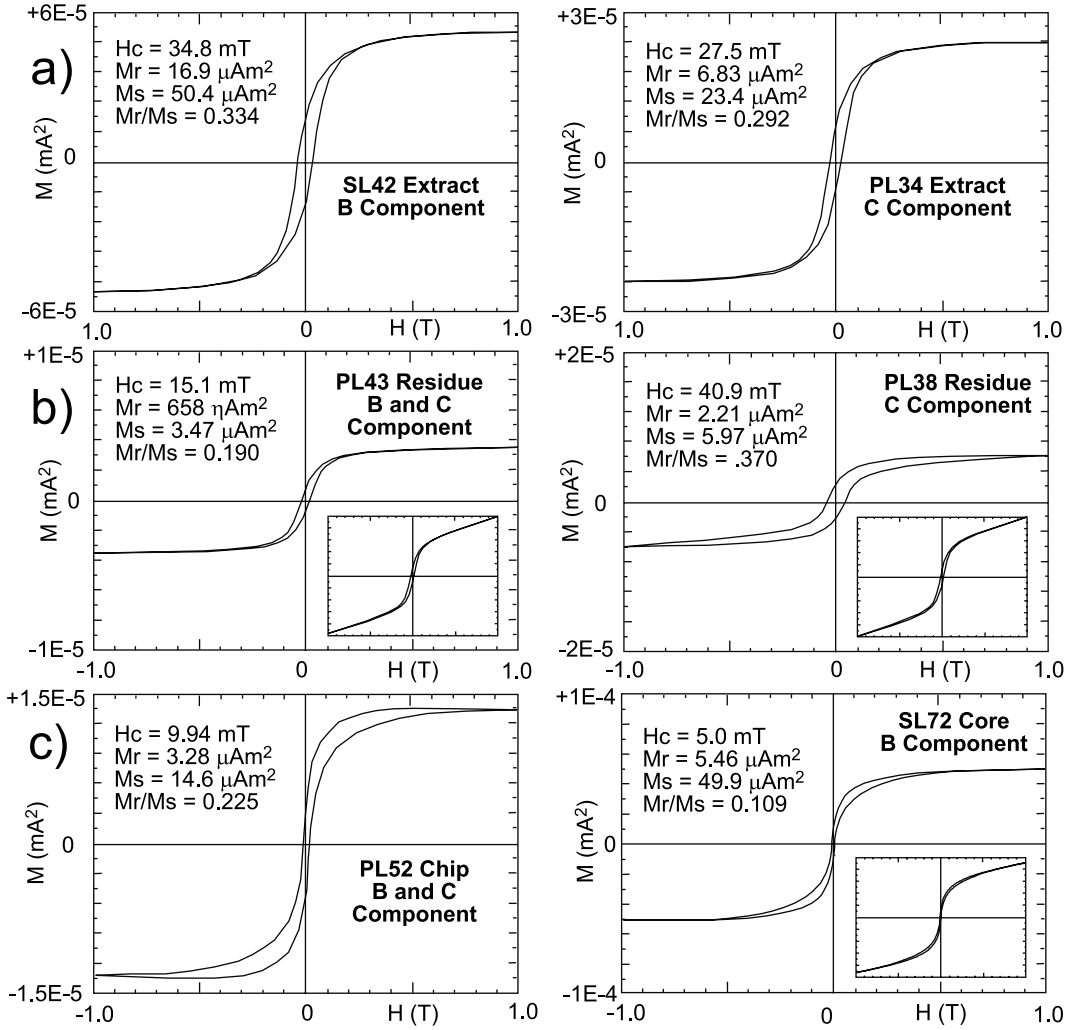

Figure 7. Typical examples of slope corrected hysteresis loops from (a) extract, (b) nonmagnetic residue, and (c) whole rock chips showing pronounced wasp-waisting. Boxes show uncorrected hysteresis loops, which indicate a strong paramagnetic influence at high field strengths.

is attained suggests that magnetite is the dominant remanence carrier [*Symons and Cioppa*, 2000].

[25] *Dunlop* [1983] documented that the shape of IRM decay curves (convex or inflected) is a characteristic signature of magnetic domain state, where convex, or exponential-like, curves represent MD magnetite grains, and inflected curves represent SD and PSD magnetite grains. In all CAA samples measured, IRM decay curves showed an inflected shape with an initial convex upward form, then a convex downward form, representative of SD and PSD behavior.

[26] ARM/IRM ratios were also calculated for CAA carbonate samples (see Table A1), with almost all samples having ratios exceeding 0.10. *Jackson et al.* [1992] found that these high ratios are typical of remagnetized North American carbonates, compared with much lower values for unremagnetized carbonates. They showed that this was a robust indicator of the presence of a large volume of very fine-grained magnetite spanning the SP-SD domain threshold.

4.5. SEM Results

4.5.1. SEM observations of thin sections. [27] Polished thin sections of CAA carbonates yielded two morphologic groups of Fe sulfides and three morphologic groups of Fe oxides. The two Fe-sulfide groups were (1) framboid spherules (Figures 11a and 11b) and (2) large euhedral grains (Figure 11a). The three Fe-oxide groups were (1) spherules (Figure 11c), (2) Fe oxide as a result of Fe-sulfide oxidation (Figure 11d), and (3) submicrometer Fe oxides associated with authigenic minerals (Figures 11e, 11f, and 11g). The oxides and sulfides observed were almost exclusively present along grain boundaries (e.g. calcite, quartz, dolomite, and clays), within cavities, or associated with fractures and veins (Figures 11a, 11b, and 11d–11g). Very rarely was an oxide or sulfide observed within apparently undisturbed calcite grains. A rare exception is found in Figure 11c.

[28] Framboid spherules made up the largest concentration of Fe sulfides in thin section (Figure 11c), recognized by their aggregate crystal form of well-defined octahedral and cubo-octahedral crystals. As also observed by *Suk et al.* [1993], framboid spherules were almost always perfectly round, with occasional irregularly shaped aggregates. The framboid spherules yielded EDS spectra of pure Fe with a significant S peak.

[29] The most abundant pure Fe oxide observed in thin section was Fe oxide replacement of Fe sulfide as spherules, single crystals, or crystal aggregates (Figures 11c and 11d). The individual crystals that made up the spherules and aggregates were usually <1 μm in diameter but sometimes up to 10 μm, either consisting of Fe-oxide rims with Fe-sulfide cores, Fe-oxide crystals with hollow

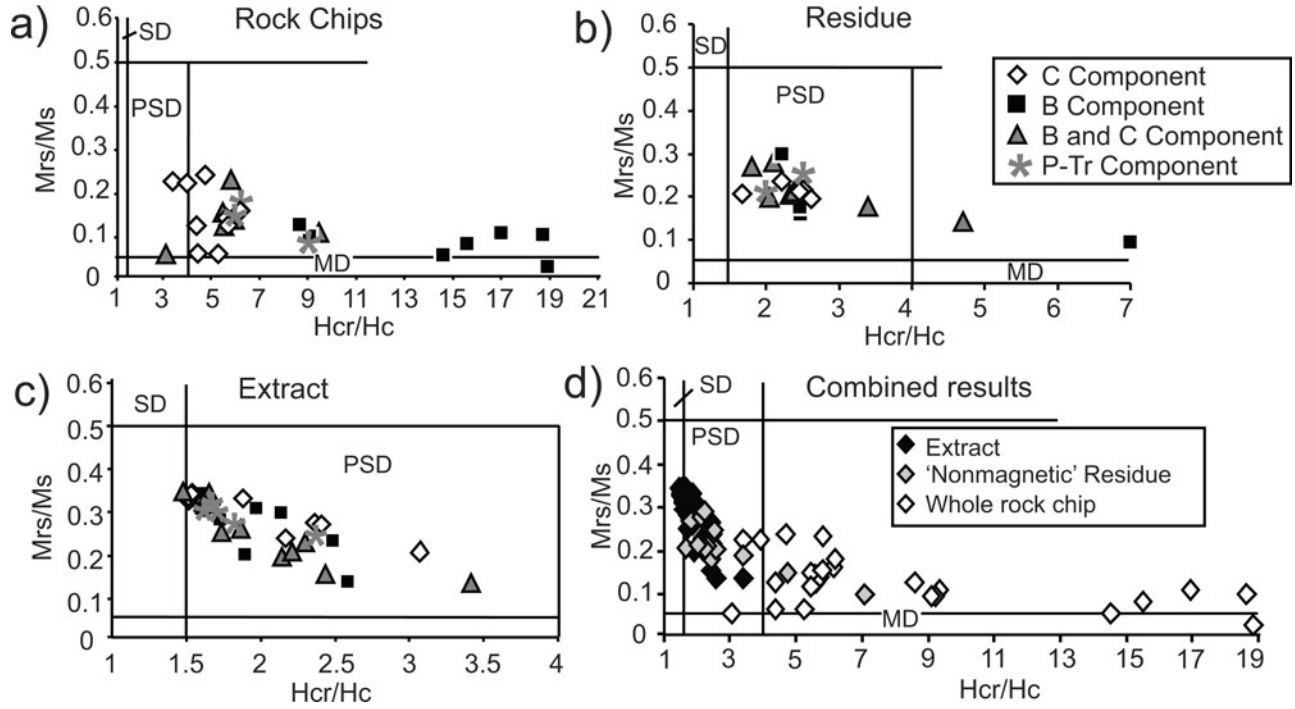

Figure 8. Hysteresis ratios plotted according to *Day et al.* [1977] for (a) whole rock chips, (b) nonmagnetic residue, and (c) extract. The samples that carry the C component are represented by diamonds, the B component by squares, the B plus C components by triangles, and the PT component by asterisks. (d) Hysteresis ratios for all data showing trend from high Hcr/Hc and low Mrs/Ms ratios for whole rock data (open diamonds) toward low Hcr/Hc and higher Mrs/Ms ratios for nonmagnetic residue (shaded diamonds) and extract data (solid diamonds).

cores, or solid Fe-oxide crystals. Similar observations of Fe-sulfide oxidation reactions have been found in remagnetized North American carbonates [*Suk et al.*, 1990a, 1990b].

[30] Pure Fe oxides were also found in association with authigenic minerals such as dolomite and illite. Figures 11e and 11f show large iron-rich clay grains, likely smectite, within larger veins of Fe-deficient clay, dominantly illite. Associated with the alteration of smectite to illite are fine-grained Fe oxides found along clay grain boundaries and at the contact between the alteration product (illite) and the carbonate host rock. Figure 11g shows a zoned dolomite crystal (dark bands are dolomite, and light bands are dedolomite) with submicron Fe oxides concentrated within the lighter zones; however, the individual crystals that make up the Fe-oxide concentrate are too small to determine their exact cation composition with EDS. This phenomenon was found in isolated areas. In cogenetic association with the altered dolomite were spherules that had been oxidized from Fe sulfide to pure Fe oxide (Figure 11c). Moving away from the altered dolomite crystals, spherules become more sulfide rich, until only Fe-sulfide framboid spherules were found. In these areas the zoned dolomite crystals were unaltered, with dark bands of pure dolomite and lighter bands of dolomite with a measurable amount of iron (Figure 11h).

[31] The Fe oxides associated with both authigenic minerals and pyrite replacement were always found in association with cracks, veins, grain boundaries, and other likely fluid pathways. When Fe-oxide grains were large enough, EDS analysis revealed Fe as the only detectable cation.

4.5.2. SEM observations of magnetic extract. [32] Magnetic extract from CAA carbonates yielded two morphologic groups of Fe sulfides and three different morphologic groups of Fe oxides. The three Fe-oxide groups were (1) 5- to 100-μm spherules, (2) 0.1- to 5.0-μm semieuhedral to euhedral authigenic grains, and (3) 5- to 100-μm subangular to subrounded detrital grains. The two Fe-sulfide groups were (1) 5- to 50-μm framboid spherules and (2) 5- to 20-μm semieuhedral to euhedral authigenic grains.

[33] Extracted Fe-bearing spherules from CAA carbonates were characterized by several distinct surface textures: (1) smooth, (2) dendritic, and (3) platy (Figures 12a–12d). A similar variety of surface textures have been observed in previous studies of remagnetized carbonates [e.g., *Freeman*, 1986; *Xu et al.*, 1994; *Suk and Halgedahl*, 1996]. A fraction of the spherules observed was broken during the extraction process and appeared hollow. Unlike the results of *Suk and Halgedahl* [1996], none of the broken spherules appeared solid, although this does not preclude their existence. EDS spectra for spherules revealed either pure Fe, or Fe with measurable amounts of Si and Al and lesser amounts of Ca and K. These non-Fe cations are likely associated with authigenic clays [*Lu et al.*, 1990], inclusions [*Suk and Halgedahl*, 1996], or a matrix that bonds individual crystals of iron oxide [*Suk and Halgedahl*, 1996]. Nickel was notably absent from spherules, arguing against an extraterrestrial origin.

[34] Framboid spherules were present in small concentrations, distinguished from spherules by the presence of sulfur. This is in strong contrast to the thin section observations, which revealed an overabundance of framboid spherules. Therefore only a small fraction of the total sulfide volume observed in thin section was probably magnetic enough to be extracted.

[35] No X-ray diffraction or scanning transmission electron microscopy (STEM) measurements were done. Consequently, it was impossible to determine the exact mineralogy of individual oxides. However, EDS spectra combined with rock magnetic observations and crystal habit strongly suggest that the oxides observed in extract with pure Fe-cation spikes are magnetite. Similar SEM observations were made in studies of North American remagnetized carbonates, which when combined with STEM analysis confirmed magnetite as the main Fe oxide [*Suk et al.*, 1990a, 1990b, 1991; *Xu et al.*, 1998].

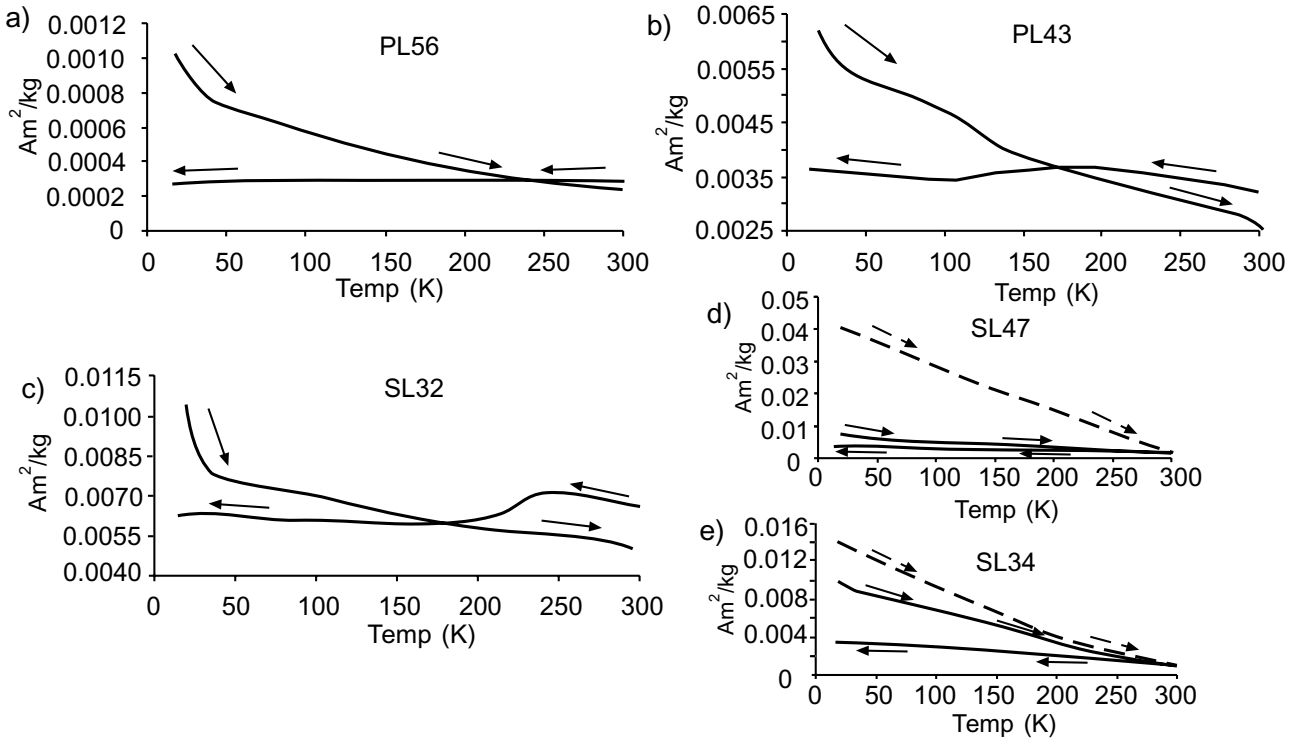

Figure 9. Representative low-temperature measurements of samples given an IRM at room temperature, allowed to cool in a zero field to 20 K, given an SIRM, and then warmed to room temperature in a zero field. (a) Example of typical behavior for most CAA samples showing rapid decay during warm-up, indicative of SP contribution to imparted IRM, (b) example of sample showing the Verwey transition at 120 K during cooldown and warm-up, and (c) example of sample showing the Morin transition soon after passing below room temperature. (d) and (e) Samples that were also field cooled in a 2.5-T field (dashed line) to test for the presence of goethite. Figure 9d confirms the three-axis IRM demagnetization of sample SL47, which showed the presence of goethite (Figure 7c). Figure 9e shows typical behavior of most samples, which show no evidence of goethite.

[36] Nonspherical Fe oxides were observed as 0.1- to 5.0-μm semieuhedral to euhedral grains (Figures 12e and 12f) and as 5- to 100-μm subangular to rounded grains (Figures 12g and 12h). EDS spectra of these particles revealed pure Fe-cation peaks. The fine-grained Fe oxides (0.1–5.0 μm) dominated the extract and were often found clustered together or coating larger grains. When the crystal form of these fine grains was large enough to discern (>1.0 μm), they were characterized by an octahedral form suggesting a magnetite mineralogy (Figures 12e and 12f). The size and crystal morphology of these particles suggest an authigenic origin.

[37] On the other hand, the very large iron oxide grains observed were all subangular to rounded, suggesting a detrital origin (Figures 12g and 12h). On several of the largest grains, botryoidal Fe-oxide overgrowth was observed, providing further evidence of authigenic magnetite crystal growth (Figure 12g). Although dominated by magnetic material, extract also included clays, sulfides, quartz, and feldspar grains and smaller populations of Ti and Cr oxides.

5. Discussion

[38] In northern Spain, Paleozoic carbonates experienced three remagnetizations temporally linked to the Late Paleozoic Variscan-Alleghanian orogeny. The NRMs of these remagnetizations have been shown, herein, to be CRMs that reside in noninteracting PSD-like magnetite. However, the presence of a large population of SP grains detected in whole rock rock magnetic properties obscures the remanence carrying population by producing a strong bimodal distribution of vastly different magnetic coercivity phases (Figure 8). This results in wasp-waisted hysteresis loops and high Hcr/Hc ratios for whole rock samples, giving CAA carbonates a remagnetization fingerprint similar to that found in North American carbonates [e.g., *Jackson*, 1990; *McCabe and Channell*, 1994]. The main cause of this bimodal distribution in CAA carbonates, when not shown to be caused by the presence of a high-coercivity mineral phase, is shown to be a mixture of SP magnetite with SD and PSD magnetite.

[39] Although not the actual remanence carrier, the abundant volume of SP grains is paradoxically the most informative and influential bulk rock magnetic characteristic of CAA carbonates. Hysteresis ratios (Figure 8), low-temperature behavior (Figure 9), and high ARM/IRM ratios all indicate that SP grains make up the largest volume of magnetic material present in CAA carbonates. However, this very fine grained material apparently does not survive the magnetic extraction process, either because of removal while decanting the acid solution or by being dissolved. The loss of SP grains is most apparent in the trend of hysteresis ratios from low Mr/Ms and higher Hcr/Hc values in whole rock measurements toward higher Mr/Ms and low Hcr/Hc values in extract measurements as the carbonate samples progress through the dissolution and extraction process (Figure 8d). This is further corroborated by the appearance of strongly wasp-waisted hysteresis loops in all whole rock samples, whereas all extract samples have nonconstricted PSD-like hysteresis loops (Figures 7a and 7c). Because SP and near SP grains have the ability to quickly change magnetization directions in low fields, they exert a strong control over Hc and Mrs/Ms values [*Suk and Halgedahl*, 1996]. Consequently, the more SP grains in a sample, the lower the sample's Hc value, and thus the higher the Hcr/Hc ratio relative to an expected Mrs/Ms ratio. This is the case in all CAA whole

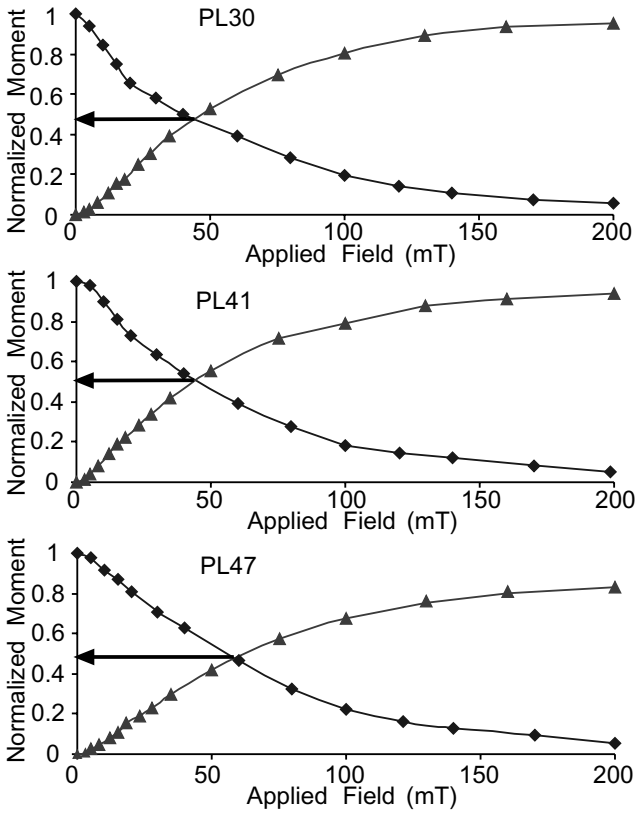

Figure 10. IRM acquisition (triangles) and AF demagnetization (diamonds) curves for representative CAA samples, indicating remanence carried by noninteracting fine particles [*Cisowski*, 1981].

rock samples. These results contradict previous studies that attempted to extract representative NRM carrying material. For example, *Suk et al.* [1993] and *Sun and Jackson* [1994] found that their extraction procedure yielded a preferential loss of SD and PSD remanence carriers, resulting in lower Mr/Ms ratios for extract compared to whole rock samples, whereas the CAA extraction procedure yielded a preferential loss of SP grains while retaining viable remanence carrying SD and PSD grains. Therefore, rather than directly characterizing the remanence carrying population through rock magnetic analysis, *Suk et al.* [1993] and *Sun and Jackson* [1994] had to infer characteristics from bulk rock analysis that was heavily overprinted by the presence of SP grains.

[40] The rock magnetic influence of SP grains is also apparent in the power law trends for hysteresis ratios. Figure 13 shows hysteresis ratios from this study compared with published trends from remagnetized North American limestones [*Channell and McCabe*, 1994; *Jackson*, 1990], unremagnetized Maiolica limestones [*McCabe and Channell*, 1994], and the results of *Parry* [1982] for synthetic magnetite mixtures. The CAA hysteresis values are noticeably different from those classically associated with remagnetized North American carbonates [e.g., *Jackson*, 1990; *Channell and McCabe*, 1994]. However, CAA whole rock data do yield a shallow power law slope similar to those of previous studies of remagnetized carbonate, albeit with lower Mrs/Ms values at the lower Hcr/Hc end. On the other hand, our extract data yield almost the same slope and y-intercept as the mixing trend of *Parry* [1982] and unremagnetized Maiolica limestones [*McCabe and Channell*, 1994]. These results suggest that the remagnetization fingerprint trend widely reported for North American carbonates [e.g., *Jackson*, 1990; *Channell and McCabe*, 1994] is paradoxically the strong influence of authigenic SP grains on whole rock hysteresis behavior and that the actual remanence carrying material, as represented by CAA extract, is almost identical to that expected for a natural mixture of SD, PSD, and MD magnetite grains.

[41] The effect of SP grains is further evidenced by the different clustered distributions of whole rock hysteresis measurements for samples carrying different CAA remagnetization components (Figure 8). Samples with the B component have the highest Hcr/Hc ratios, and by inference the largest volume of (authigenic) SP grains. The samples with the C and PT components have much lower Hcr/Hc components, and by inference a smaller volume of (authigenic) SP grains. Therefore the CAA's Late Paleozoic remagnetization history can be thought of as a series of unique and successive events, each one initiating growth of new magnetic grains. This is a similar finding to *Katz et al.* [2000], who reported an increase in the relative abundance of SP magnetite with an increased level of remagnetization. In the case of CAA carbonates the multiple remagnetization events left a fingerprint on the whole rock magnetic properties, which is now observable in their individual component's hysteresis properties. This fingerprint indicates that the abundance of SP grains is a very important consequence and characteristic of the remagnetization process in CAA carbonates and that new magnetic mineral growth is an integral component of this process.

[42] SEM observations, linked with rock magnetic results, provide further insights into the remagnetization process and the genesis of the magnetic grains responsible for chemical remanent magnetizations found in CAA carbonates. The most important production of new magnetic material comes from the oxidation of Fe sulfides, which results in the formation of new magnetite [*Suk et al.*, 1990a, 1990b]. There is an unmistakable similarity between the morphology and grain size of fine-grained Fe oxide (0.1–5.0 μm) observed in extract, to that observed as a product of Fe-sulfide replacement in thin sections. Thus it is likely that a majority of the remanence carrying PSD-like magnetite determined from rock magnetic analysis is a direct product of Fe-sulfide alteration due to oxidizing fluids. Similar observations in remagnetized New York carbonates led *Suk et al.* [1990a, 1990b] to conclude that the remagnetizations were a CRM acquired by alteration of pyrite in the presence of fluids.

[43] The importance of fluids is further confirmed by the location of alteration products (i.e., clay and dolomite) along fluid pathways such as cracks, grain boundaries, and interconnected voids. Additionally, the abundant submicron Fe oxides found in cogenetic relationship with these authigenic mineral phases gives further evidence for fluid involvement in the remagnetization process. In North American carbonates these same alteration products (dolomite and illite) have been shown to form penecontemporaneously with remagnetizations [*Elmore et al.*, 1985; *Hart and Fuller*, 1988; *Suk et al.*, 1993] and by inference both are related to the same process.

[44] Given the above SEM observations, it is apparent that the new potential remanence carrying magnetic material is a product of both new mineral nucleation and growth and oxidation of existing mineral phases. The abundance of extracted euhedral fine-grained pure Fe oxide (0.1–5.0 μm), Ni-free Fe-oxide spherules, and the presence of botryoidal iron oxide overgrowths on detrital grains in CAA magnetic extracts confirm thin section observations that the majority of magnetic material present in CAA carbonates is authigenic in origin. Furthermore, the cogenetic relationship between Fe oxides and fluid pathways and alteration products (e.g., illite and dolomite) indicates that the authigenic reactions that produced the aforementioned Fe oxides

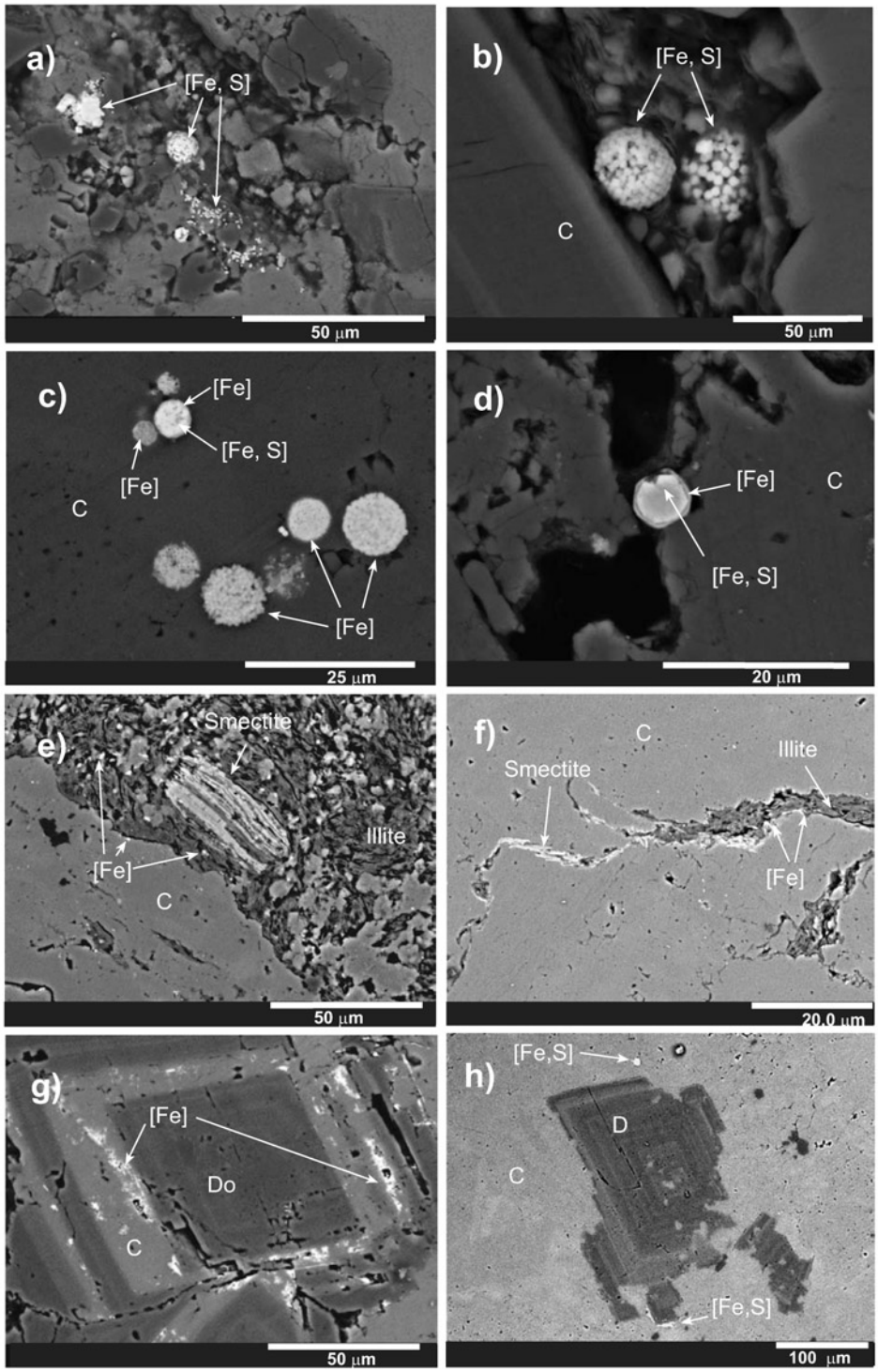

Figure 11. Backscattered SEM images of CAA carbonate thin sections. (a) and (b) Secondary Fe-sulfide framboid spherules and single euhedral Fe-sulfide crystals located within void space and along cracks. (c) A Fe-sulfide framboid spherule and several Fe-oxide spherules (oxidized Fe sulfide) found in close approximation with dedolomite in Figure 11g. (d) Large single Fe-sulfide crystal showing an oxidized rim of Fe oxide located within a microfracture. (e) and (f) Micron-scale Fe oxides associated with Fe-rich clay (smectite) within large veins of Fe-deficient clay (illite). (g) A zoned dolomite (darker bands) and dedolomite (lighter bands) crystal with submicron Fe oxides concentrated within the dedolomite zones. (h) A mostly unaltered dolomite crystal associated with several Fe-sulfide framboid spherules. The lighter zones of the dolomite crystal have measurable amounts of Fe present.

occurred in the presence of fluids. The likely source of iron in these fluids comes either from transformation of Fe-rich clays (e.g., smectite, chlorite) to illite [*Jackson et al.*, 1988; *Lu et al.*, 1991; *Katz et al.*, 1998b], from alteration of organic rich sediment [*Katz et al.*, 1998a], from alteration of originally ferruginous carbonate material [*Bachtadse et al.*, 1987], or from alteration and dissolution of Fe sulfides or detritus material such as chromite, iron-titanium oxides, etc. Additional iron could also have been transported into the carbonate system by externally derived fluids.

[45] The above mentioned need for fluids in the formation of the authigenic magnetite requires a fluid source. The source of these fluids has been the subject of debate in most studies of remagnetized carbonates. The two main sources for fluids are thought to be localized pore fluids [*Elmore et al.*, 1993] or externally derived fluids [*Oliver*, 1986; *Bethke and Marshak*, 1990]. Because of the contemporaneous nature of remagnetization and orogenesis, most studies of Late Paleozoic remagnetizations have called upon tectonically driven fluids for authigenic activation. Tectonically driven fluids can be activated by large-scale thrusting and deformation in the hinterland, which acts as a "squeegee" to drive fluids toward the foreland [*Oliver*, 1986]. Such a model has been used to explain the occurrence of hydrocarbons and Mississippi Valley-type deposits in the Appalachian foreland. Tectonic fluids can also be activated by gravity-driven flow of meteoric water due to topographically enhanced structural stacking within an orogenic deformation zone [*Bethke*, 1986]. Without further geochemical analysis of fluid inclusions and isotopic composition from CAA carbonates, the exact origin of the fluids (meteoric, formational, or brinal) responsible for CAA remagnetizations remains speculative. However, the coeval nature of remagnetizations with different deformation events in the CAA's tectonic history [*Weil et al.*, 2000], indicates that tectonism was the catalyst for fluid flow, and consequently, was the underlying cause of remagnetization.

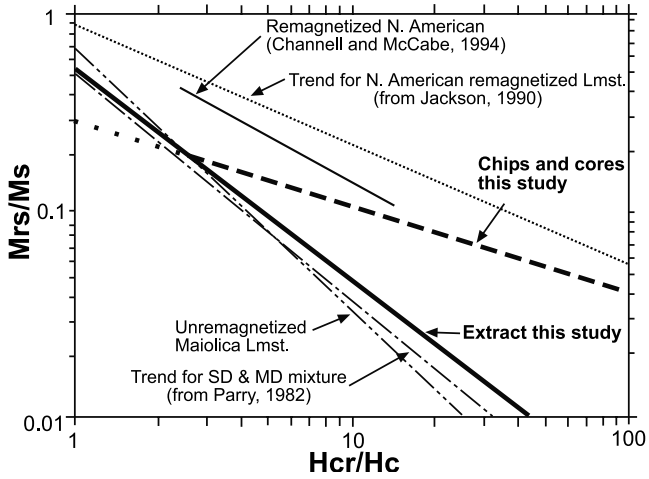

Figure 13. Best fit power law trends for hysteresis ratios from CAA carbonate whole rock (heavy dashed line) and extract data (heavy solid line) compared with published trends from remagnetized North American carbonates (dotted line, *Jackson* [1990]; thin solid line, *Channell and McCabe* [1994]), unremagnetized Maiolica carbonates (dashed-double dotted line, *Channell and McCabe* [1994]), and the results of *Parry* [1982] (dashed-single dotted line) for synthetic mixtures of magnetite.

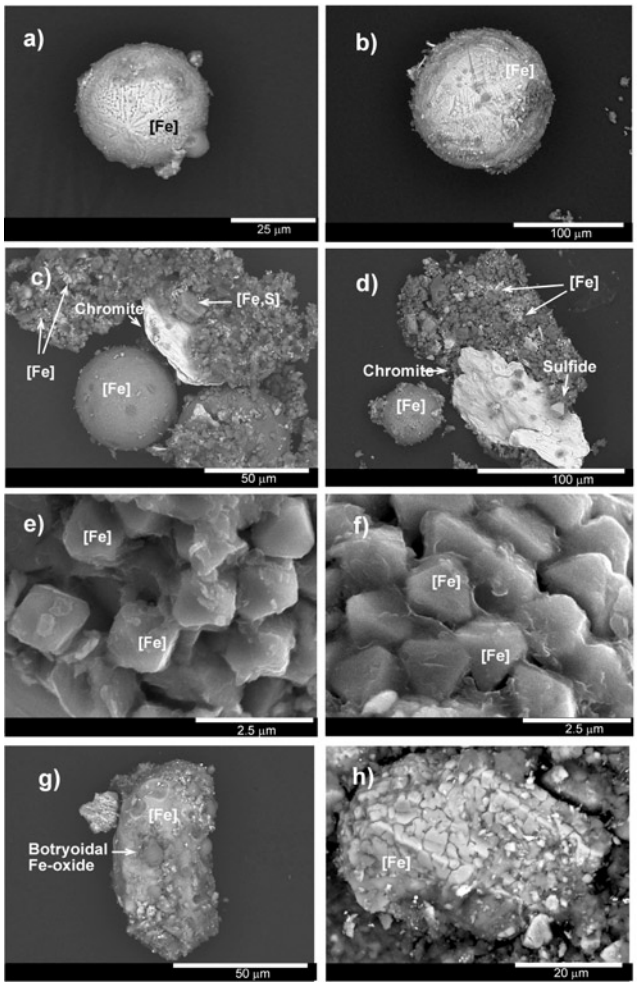

Figure 12. Backscattered and secondary-electron SEM images of CAA magnetic extract. (a) and (b) Pure Fe-oxide spherules coated with fine clay and Fe-oxide particles. (c) and (d) Pure Fe-oxide spherules with abundant clustered fine-grained Fe oxides, large detrital chromite grains, and large euhedral sulfide crystals. (e) and (f) Very fine grained euhedral Fe-oxide crystals coated with a thin film of clay. (g) A large rounded detrital Fe-oxide grain with secondary botryoidal overgrowth of Fe oxide. (h) A large subangular detrital Fe-oxide grain that has undergone dissolution.

6. Conclusions

[46] Together, SEM observations and rock magnetic experiments reveal that the three Late Paleozoic remagnetizations experienced by CAA Paleozoic carbonates are CRMs facilitated by the presence of fluids. We conclude that the fluids, whether externally or internally derived, are activated as a response to tectonism because of the synchroneity of the remagnetizations with the local Variscan-Alleghanian orogenic phases. The corresponding megascale tectonic event likely increased fluid mobility, as a product of tectonic thickening (thrust sheet stacking), tectonically induced permeability, and/or gravity-driven flow, which ultimately facilitated the growth of new magnetic material. In CAA carbonates, fluid flow driven chemical reactions resulted in the formation of submicron to micron-sized Fe oxide associated with Fe-rich clay and calcite-dolomite alteration, or as oxidation of Fe-sulfide framboids to form magnetite. This newly formed PSD-like magnetite, which has similar rock magnetic characteristics to those found in unremagnetized carbonates, is the dominant remanence carrying material. However, the most striking rock magnetic characteristic of CAA carbonates, and thus their fingerprint, is paradoxically the large population of SP magnetite that grew during the remagnetization events and not the newly formed remanence carrying material.

[47] **Acknowledgments.** We would like to thank Douglas Elmore, Pierrick Roperch, Andrei Kosterov, and an anonymous reviewer for their helpful comments, which greatly improved the quality of this manuscript. Some of this research was made possible by a Visiting Fellowship at the Institute for Rock Magnetism (IRM) at the University of Minnesota. The IRM is funded by the Instruments and Facilities Program, Earth Sciences Division, National Science Foundation, and the W. M. Keck Foundation. This study is supported by the National Science Foundation, Division of Earth Sciences, grant EAR-9804765.

References

Bachtadse, V., R. Van der Voo, F. M. Haynes, and S. E. Kesler, Late Paleozoic magnetization of mineralized and unmineralized Ordovician carbonates from east Tennessee: Evidence for a post-ore chemical event, *J. Geophys. Res.*, *92*, 14,165–14,176, 1987.

Bando, Y., M. Kiyama, N. Yamamoto, T. Takada, T. Shinjo, and H. Takaki, Magnetic properties of α-Fe_2O_3 fine particles, *J. Geophys. Soc. Jpn.*, *20*, 2086, 1965.

Bastida, F., C. Brime, S. Garcia-Lopez, and G. N. Sarmiento, Tectonothermal evolution in a region with thin-skinned tectonics: The western nappes in the Cantabrian Zone (Variscan Belt of NW Spain), *Int. J. Earth Sci.*, *88*, 38–48, 1999.

Bethke, C. M., Hydrologic constraints of the genesis of upper Mississippi Valley mineral district from Illinois basin brines, *J. Econ. Geol.*, *81*, 233–249, 1986.

Bethke, C. M., and S. Marshak, Brine migration across North America—The plate tectonics of groundwater, *Annu. Rev. Earth Sci.*, *18*, 287–315, 1990.

Channell, J. E. T., and C. McCabe, Comparison of magnetic hysteresis parameters of unremagnetized and remagnetized limestones, *J. Geophys. Res.*, *99*, 4613–4623, 1994.

Cisowski, S., Interacting vs. non-interacting single domain behavior in natural and synthetic samples, *Phys. Earth Planet. Inter.*, *26*, 56–62, 1981.

Day, R., M. Fuller, and V. A. Schmidt, Hysteresis properties of titanomagnetites: Grain-size and compositional dependence, *Phys. Earth Planet. Inter.*, *13*, 260–267, 1977.

Dunlop, D., Determination of domain structure in igneous rocks by alternating field methods, *Earth Planet. Sci. Lett.*, *63*, 353–357, 1983.

Elmore, R. D., W. Dunn, and C. Peck, Absolute dating of dedolomitization by means of paleomagnetic techniques, *Geology*, *13*, 558–561, 1985.

Elmore, R. D., D. London, D. Bagley, D. Fruit, and G. Gao, Remagnetization by basinal fluids: Testing the hypothesis in the Viola Limestone, southern Oklahoma, *J. Geophys. Res.*, *98*, 6237–6254, 1993.

Freeman, R., Magnetic mineralogy of pelagic limestones, *Geophys. J. R. Astron. Soc.*, *85*, 433–452, 1986.

Hart, M., and M. Fuller, Magnetization of a dolomite bed in the Monterey Formation: Implications for diagenesis, *Geophys. Res. Lett.*, *15*, 491–494, 1988.

Jackson, M., Diagenetic sources of stable remanence in remagnetized Paleozoic cratonic carbonates: A rock magnetic study, *J. Geophys. Res.*, *95*, 2753–2761, 1990.

Jackson, M., C. McCabe, M. Ballard, and R. Van der Voo, Magnetite authigenesis and diagenetic paleotemperatures across the northern Appalachian Basin, *Geology*, *16*, 592–595, 1988.

Jackson, M., W. W. Sun, and J. P. Craddock, The rock magnetic fingerprint of chemical remagnetization in midcontinental Paleozoic carbonates, *Geophys. Res. Lett.*, *19*, 781–784, 1992.

Katz, B., R. D. Elmore, and M. H. Engel, Authigenesis of magnetite in organic-rich sediment next to a dike: Implications for thermoviscous and chemical remagnetizations, *Earth Planet. Sci. Lett.*, *163*, 221–234, 1998a.

Katz, B., R. D. Elmore, M. Cogoini, and S. Ferry, Widespread chemical remagnetization: Orogenic fluids or burial diagenesis of clays?, *Geology*, *26*, 603–606, 1998b.

Katz, B., R. D. Elmore, M. Cogoini, H. E. Michael, and S. Ferry, Associations between burial diagenesis of smectite, chemical remagnetization, and magnetite authigenesis in the Vocontian trough, SE France, *J. Geophys. Res.*, *105*, 851–868, 2000.

Kent, D. V., Thermoviscous remagnetization in some Appalachian limestones, *Geophys. Res. Lett.*, *12*, 805–808, 1985.

Liebermann, R. C., and S. K. Banerjee, Magnetoelastic interactions in hematite: Implications for geophysics, *J. Geophys. Res.*, *76*, 2735–2756, 1971.

Lowrie, W., Identification of ferromagnetic minerals in a rock by coercivity and unblocking temperature properties, *Geophys. Res. Lett.*, *17*, 159–162, 1990.

Lu, G., S. Marshak, and D. Kent, Characteristics of magnetic carriers responsible for Late Paleozoic remagnetizations in carbonate strata of the mid-continent, U.S.A., *Earth Planet. Sci. Lett.*, *99*, 351–361, 1990.

Lu, G., C. McCabe, J. S. Hanor, and R. E. Ferrell, A genetic link between remagnetization and potassic metasomatism in the Devonian Onondaga Formation, northern Appalachian Basin, *Geophys. Res. Lett.*, *18*, 2047–2050, 1991.

McCabe, C., and J. E. T. Channell, Late Paleozoic remagnetization in limestones of the Craven Basin (northern England) and the rock magnetic fingerprint of remagnetized sedimentary carbonates, *J. Geophys. Res.*, *99*, 4603–4612, 1994.

McCabe, C., R. Van der Voo, D. R. Peacor, C. R. Scotese, and R. Freeman, Diagenetic magnetite carries ancient yet secondary remanence in some Paleozoic sedimentary carbonates, *Geology*, *11*, 221–223, 1983.

Molina-Garza, R. S., and J. D. A. Zijderveld, Paleomagnetism of Paleozoic strata, Brabant and Ardennes Massifs, Belgium: Implications of prefolding and postfolding Late Carboniferous secondary magnetizations for European polar wander, *J. Geophys. Res.*, *101*, 15,799–15,818, 1996.

Morrish, A. H., *Canted Antiferromagnetism: Hematite*, 192 pp., World Sci., Singapore, 1994.

Muttoni, G., "Wasp-waisted" hysteresis loops from a pyrrhotite and magnetite-bearing remagnetized Triassic limestone, *Geophys. Res. Lett.*, *22*, 3167–3170, 1995.

Oliver, J., Fluids expelled tectonically from orogenic belts: Their role in hydrocarbon migration and other geologic phenomena, *Geology*, *14*, 99–102, 1986.

Özdemir, O., and D. J. Dunlop, Intermediate magnetite formation during dehydration of goethite, *Earth Planet. Sci. Lett.*, *177*, 59–67, 2000.

Parés, J., R. Van der Voo, and J. A. Stamatakos, Palaeomagnetism of Permian and Triassic red beds of NW Spain and implications for the tectonic evolution of the Asturian-Cantabria Arc, *Geophys. J. Int.*, *126*, 893–901, 1996.

Parry, L. G., Magnetization of immobilized particle dispersions with two distinct particle sizes, *Phys. Earth Planet. Inter.*, *28*, 230–241, 1982.

Pick, T., and L. Tauxe, Holocene paleointensities: Thellier experiments on submarine basaltic glass from the East Pacific Rise, *J. Geophys. Res.*, *98*, 17,949–17,964, 1993.

Raven, J. G. M., and B. A. Van der Pluijm, Metamorphic fluids and transtension in the Cantabria Mountains of northern Spain: An application of the conodont color alteration index, *Geol. Mag.*, *123*, 673–681, 1986.

Roberts, A., Y. Cui, and L. Verosub, Wasp-waisted hystersis loops: Mineral magnetic characteristics and discrimination of components in mixed magnetic systems, *J. Geophys. Res.*, *100*, 17,909–17,924, 1995.

Suk, D., and S. Halgedahl, Hysteresis properties of magnetite spherules and whole rock specimens from some Paleozoic platform carbonate rocks, *J. Geophys. Res.*, *101*, 25,053–25,075, 1996.

Suk, D., D. R. Peacor, and R. Van der Voo, Replacement of pyrite framboids by magnetite in limestones and implications for paleomagnetism, *Nature*, *345*, 611–613, 1990a.

Suk, D., R. Van der Voo, and D. R. Peacor, Scanning and transmission electron observations of magnetite and other iron phases in Ordovician carbonates from east Tennessee, *J. Geophys. Res.*, *95*, 12,327–12,336, 1990b.

Suk, D., R. Van der Voo, and D. R. Peacor, SEM/STEM observations of magnetite in carbonates of eastern North America: Evidence for chemical remagnetization during the Alleghenian orogeny, *Geophys. Res. Lett.*, *18*, 939–942, 1991.

Suk, D., R. Van der Voo, and D. R. Peacor, Origin of magnetite responsible for remagnetization of early Paleozoic limestones of New York State, *J. Geophys. Res.*, *98*, 419–434, 1993.

Sun, W., and M. Jackson, Scanning electron microscopy and rock magnetic studies of magnetite carriers in remagnetized early Paleozoic carbonates from Missouri, *J. Geophys. Res.*, *99*, 2935–2942, 1994.

Symons, D. T. A., and M. T. Cioppa, Crossover plots: A useful method for plotting SIRM data in paleomagnetism, *Geophys. Res. Lett.*, *27*, 1779–1782, 2000.

Tauxe, L., T. A. T. Mullender, and A. Pick, Potbellies, wasp-waists, and superparamagnetism in magnetic hysteresis, *J. Geophys. Res.*, *101*, 571–583, 1996.

Thominski, H. P., J. Wohlenberg, and U. Bleil, The remagnetization of Devono-Carboniferous sediments from the Ardennes-Rhenish Massif, Germany, *Tectonophysics*, *225*, 411–431, 1993.

Van der Voo, R., J. A. Stamatakos, and J. M. Parés, Kinematic constraints on thrust-belt curvature from syndeformational magnetizations in the Lagos del Valle Syncline in the Cantabrian Arc, Spain, *J. Geophys. Res.*, *102*, 10,105–10,120, 1997.

Wasilewski, P. J., Magnetic hysteresis in natural materials, *Earth Planet. Sci. Lett.*, *20*, 67–72, 1973.

Weil, A. B., R. Van der Voo, B. A. van der Pluijm, and J. M. Parés, Unraveling the timing and geometric characteristics of the Cantabria-Asturias Arc (northern Spain) through paleomagnetic analysis, *J. Struct. Geol.*, *22*, 735–756, 2000.

Weil, A. B., R. Van der Voo, and B. van der Pluijm, Oroclinal bending and evidence against the Pangea megashear: The Cantabria-Asturias Arc (northern Spain), *Geology*, *29*, 991–994, 2001.

Xu, W. , R. Van der Voo, and D. R. Peacor, Are magnetite spherules capable of carrying stable magnetizations?, *Geophys. Res. Lett.*, *21*, 517–520, 1994.

Xu, W., R. Van der Voo, and D. Peacor, Electron microscopic and rock magnetic study of remagnetized Leadville carbonates, central Colorado, *Tectonophysics*, *296*, 333–362, 1998.

R. Van der Voo, Department of Geological Sciences, University of Michigan, Ann Arbor, MI 48103, USA. (voo@umich.edu)

A. B. Weil, Department of Geology, Bryn Mawr College, 101 N. Merion Ave., Bryn Mawr, PA 19010, USA. (aweil@byrnmawr.edu)